Proceedings World Geothermal Congress 2020+1
Reykjavik, Iceland, April - October 2021

Optimizing Geothermal Energy Storage in Harsh Conditions

Teppo Arola, Petri Hakala, Sami Vallin

Geological Survey of Finland. PO Box 96, Vuorimiehentie 5, FI-02151 Espoo, Finland

teppo.arola@gtk.fi

Keywords: BTES, cold climate, simulation, field measurements, Finland

ABSTRACT

A novel hybrid geothermal energy storage was modelled, built and started to be monitored in Central Finland. Large amount of waste heat is produced by compressors in the industrial process. Waste heat is collected and transformed to the optimized and monitored borehole thermal energy storage (BTES) which is located under oat field. Solar heat is also used to charge the heat storage during summer. The primary user for this waste and stored heat is a local swimming bath near a factory. Ground temperatures during the operation will be monitored continuously. Hence, it is possible to optimize BTES charging and utilization even during operation.

The BTES was planned and optimized using Comsol Multiphysics modelling software. Undisturbed average ground temperature is approximately 5 °C on the area. Ground is charged at the fluid temperature of 70 °C and utilized until temperature will drop to 20 °C. Charging time is 24 hours for 150 days followed by 120 days of energy utilization time. The BTES is monitored by temperature sensors located in the borehole heat exchangers and optic measuring cable which is installed to the top and the bottom of the topmost insulation layer.

As a result, the most optimal BTES solution was considered to be hexagonal shaped energy well field which has 61 energy wells of 45 meters depth. The distance between boreholes is approximately 2.5 m. The BTES consist four energy well circles which will be charged and discharged according to the current ground and waste heat fluid temperatures. All wells are equipped with 40 mm borehole heat exchanger pipes with thickened wall. Due to cold climatic conditions, insulation layer is needed for the uppermost part of the BTES. This configuration provides that the temperature may rise approximately to 67°C in the middle of BTES and it is possible to utilize instantaneous power of 150 kW. The BTES efficiency will increase every year and will achieve the level of 60% during ten years of operation.

Due to the short operating time only preliminary field data is available. According to the field measurement the subsurface temperature evolution is close to the values predicted by the simulations on the middle part of the BTES but on the peripheral area measured temperature is lower than simulated.

Our simulation and preliminary temperature measurements reveals that it is possible to plan and built efficient BTES on the harsh climatic condition. The knowledge of local thermogeological factors is essential. Climatological requirements have to be taken into account when planning, construct and operate the system. More information from temperature measurements and temperature sensor development work is needed in the future. It is also important to report different international underground energy storage projects to increase the knowledge of geothermal storage possibilities and hence increase the heat recycling to reduce greenhouse gas emissions.

1. INTRODUCTION

Mounting concerns of climate change has addressed political decision makers to act towards more renewable energy production in many countries (e.g. Ge et al. 2019; Valkila et al. 2010). European Union has been an active player in international climate discussion for many years. For example, the European Climate Foundation, ECF, (2010) has developed the “Energy Road Map”, and published several reports and notifications under the “Net Zero 2050” project to find solutions for reducing greenhouse gas emissions to net-zero by 2050 (e.g. ECF, 2018; 2019).

Geothermal energy is one well known area of renewable energy production. Geothermal energy utilization for heating has been continuously increasing in Europe (Dumas et al. 2019). The low enthalpy energy utilization, named as shallow geothermal energy, is the most extensively used geothermal resource in the Nordic countries, excluding Iceland. Shallow geothermal refers to energy utilization from relatively shallow depths; 100 to 400 m below ground level, and most often a heat pump is needed to arise the fluid temperature at a rational level for heating purposes. The low surface temperature, thermal gradient and heat flow constitutes barriers to efficient geothermal heating energy production on the old continental crust areas located on Nordic hemispheres. One option to rise the heating potential is to combine geothermal energy with solar and/or industrial waste heat production. However, even if the total amount of solar and/or industrial waste heat energy is high these energy production methods are often unfavorable for direct renewable energy utilization because the energy need and the generation are not simultaneous. For example, solar power in Nordic hemispheres can be utilized efficiently on summer months when the heating demand of buildings is low and very often a large power of industrial waste heat is produced on short time cycles. Hence, heat energy storages are needed to equalize the energy production and demand. One practical and easy option is to use ground as a heating storage medium. The heat from solar and/or waste heat form industry is transferred to the ground via vertical borehole heat exchangers (BHEs) which are installed to borehole drilled to the ground. This system is called borehole thermal energy storage, BTES (Nordell, 2000). Modern BTES systems are normally operating at low temperatures, near the natural temperature of the ground, providing seasonal thermal energy storage for large buildings or industrial site (Lanahan and Tabares-Velasco, 2017; Korhonen et al., 2018; Shah et al., 2018). There are only few examples of high temperature BTES which are connected directly to district heating network (Nussbicker et al. 2007; Sibbitt et al. 2012; Bauer et al. 2016). The low ground temperature and relatively high thermal conductivity due to crystalline, quartz rich rock generates stored heat to diffuse large areas and hence reduce the efficiency of energy storage in Finland and countries with similar climatic and geological

conditions. Overburden layer, which exists mostly by thick layer of glacial till or clay in Finland may offer a better media for high temperature BTES system than bedrock.

In general, heat extraction coefficient of BTES systems is moderate in the first years due to thermal losses in cold climate conditions. However, efficiency increases every year due to elevated subsurface temperature if the amount of injected energy is higher than extracted (Schulte, 2016). Relative heat losses decrease when the volume of heat storage increases. Also BTES efficiency increases with higher charging and lower discharging inlet temperatures (Welsch et al, 2016). Catolico, et al. (2015) showed that heat extraction efficiency is better if the thermal conductivity of the ground is low because temperature gradient near the boreholes is then higher. Hence solid bedrock is more favorable than bedrock with fractures since convective heat transfer due to groundwater flow decreases the BTES efficiency.

Geological Survey of Finland (GTK) was participated in a project which aims to reduce greenhouse gas emissions by storing excess heat into the ground. In this project the stored heat is originated from an industrial process where drinking bottles are blasted from plastic billets and from 200 m^2 solar collectors which are installed on the roof of the factory. The aim of this study is to investigate whether it is possible to plan and operate a high temperature BTES where boreholes are drilled to very shallow depth to the ground in harsh climatic conditions. Our aim is to emphasize the utilization of geothermal energy storages as an option towards zero carbon communities in Nordic conditions.

2. MATERIAL AND METHODS

2.1 Site Description

The investigation was carried out on site located in Toholampi, in the Central Finland, approximately 400 km north from Helsinki (Fig.1). BTES is located in an oat field next to the Finn Spring ltd. soft drink manufactory. Geologically the uppermost layer is clay which thickness is on average 22.4 m. Directly under clay is bedrock. The site is located at the contact zone of gabbro and diorite.

According the Meteorological Institute of Finland, the average air temperature on the site was 3.6°C between 1981 and 2010 and permanent snow cover lasted 130 to 160 days per year. The average ground surface temperature is approximately 5.0 °C according to calculations made by GTK and average groundwater temperature is 5.5 °C (Hietula, 2018).

Figure 1: Location map. The capital of Finland, Helsinki and the study site are presented.

2.2 Borehole thermal energy storage (BTES)

Boreholes, including a test borehole were drilled and vertical borehole heat exchangers (BHEs) were installed in 2018. Because of the thick soil layer steel pipes were drilled and anchored to the bedrock to prevent soil disruption. Heat injection into the BTES started in the spring 2019. Heat extracted from the BTES during winter is primarily used for water heating in swimming bath near the factory. Styrofoam insulation layer with a thickness of 0.1m, was installed to the top of the BTES to prevent a) heat from escaping the ground and b) the frost formation. A single U-pipe collector is installed into each groundwater filled borehole and water is used as a heat carrier fluid inside the pipes. The inner radius of the collector in each BHE is 16.3 mm and outer 20.0 mm. Due to the high fluid temperature pipe walls are thickened. Collector type is PE-RT which resist high temperatures better than ordinary PEM and PEH collector pipes. There are no spacers between the pipe shanks. Final BTES consists of 61 boreholes with diameter of 115 mm and the depth of 45 m. Boreholes are drilled to the hexagonal pattern since simulations showed that thermal losses and dead zones between BHEs are then minimized. Distance between boreholes is nearly the same in every direction being 2.5 m.

BTES simulations were performed using finite element modelling software COMSOL Multiphysics. Temperature sensors (TERMO cable and sensors from Dimense Ltd) were installed in the water filled space inside the boreholes to actively monitor the temperature differences occurring between charging and discharging periods. Borehole field, i.e. storage volume, is divided into four rings of BHEs. Number of BHEs in different rings are 8 (ring 1), 12 (ring 2), 18 (ring 3) and 23 (ring 4) respectively (Fig. 2). Each BHE in a certain ring is connected in parallel and four rings are connected in series. Using the temperature controller developed by Heliostorage ltd. heat is charged to the ring which has optimal temperature to receive heat. For example, if the charging temperature is lower than the core temperature of the storage, outer BHE rings are charged instead of the core ring.

The fiber optic cable was installed in the bottom and upper surfaces of the Styrofoam insulation layer (Fig 2).

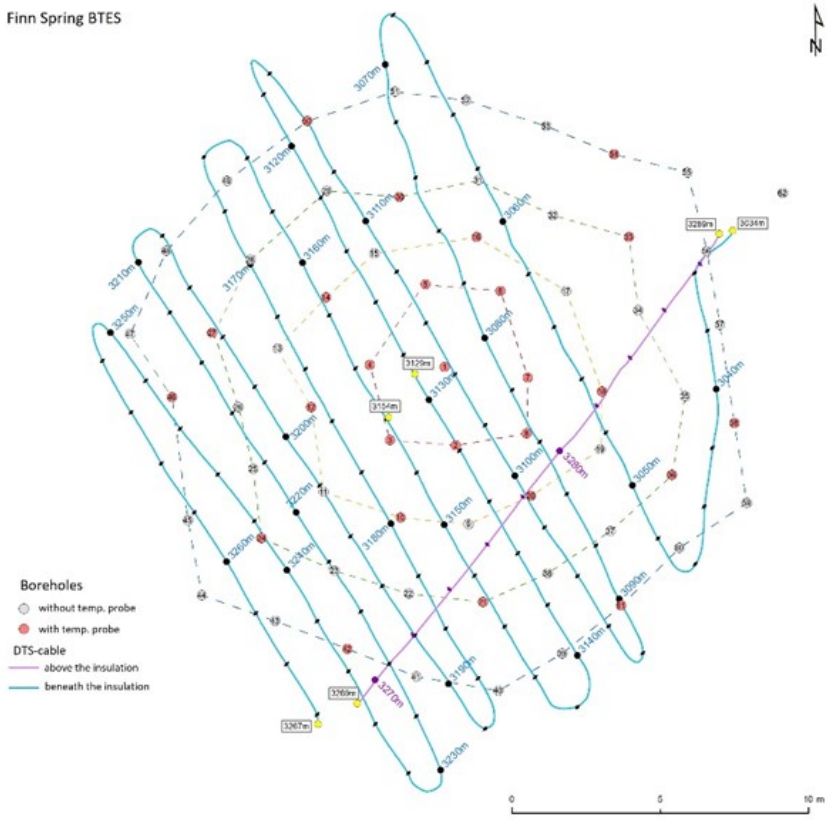

Figure 2: Layout of the BTES and locations of TERMO temperature sensors. Totally 61 boreholes (á 45 m) are drilled of which 26 are equipped with TERMO temperature probes. Optical fiber cable (DTS-cable) for temperature monitoring is installed in the upper and lower surfaces of the insulation layer (0.1 m Styrofoam).

2.3 Thermal response test and initial temperature measurement

Two conventional thermal response tests (TRT) were carried out on the site to determine the effective thermal conductivity of the subsurface and the effective thermal resistance of the borehole. The first TRT was conducted in the 60 m deep test borehole (borehole number 62 in the Fig. 2) which is not included to the operating BTES. However, the test borehole is equipped with optical fiber cable for temperature monitoring. The second TRT was performed from one of the 45 m deep boreholes included to the operating BTES. TRT-data was interpreted using analytical infinite line source method combined with temporal superposition approach. The results were used in numerical COMSOL simulations to study how subsurface temperature evolves between charging and discharging phases.

Initial temperature profile of the ground as a function of depth was measured using temperature probes Antares type 1854 miniaturized data logger and RBR duet.

2.4 Numerical model of the BTES

In COMSOL simulations, all BHEs were assumed to be strictly vertical. BTES was modelled using three-dimensional mesh grid. Due to large number of finite elements BHEs were approximated as hollow cylinders without the need for meshing the interior of the BHE. This reduced the number of finite elements significantly. The size of the modelled geometry is 90 m × 90 m × 86.5 m (Fig. 3.)

The model consist of four volume meshes. Uppermost volume (overburden above BHEs, 1.5 m), Styrofoam insulation layer (0.1 m) and bedrock volume beneath boreholes was meshed using tetrahedral elements. Horizontal surface in the interface between overburden, Styrofoam and BHEs was meshed using triangular elements with maximum growth rate of 1.3. Collars of the BHEs were meshed with edge elements whose length was 15 mm. Swept mesh was used for the remaining of the model from the upper horizontal surface of boreholes to the bottom of the boreholes as shown in the Fig. 3. Total number of elements was 938 356.

During the heat injection period the subsurface is charged at water inlet temperature of 70 °C and discharged at temperature of 20 °C. When charging, the flow direction of the heat carrier fluid is from the center (ring 1) towards the outer boundaries of the storage (ring 4). During discharge, the flow direction is reversed, fluid flows from the 4th ring towards the 1st ring. The BTES is designed so that the ground temperature should always be the highest in the middle of the storage.

a) b) c)

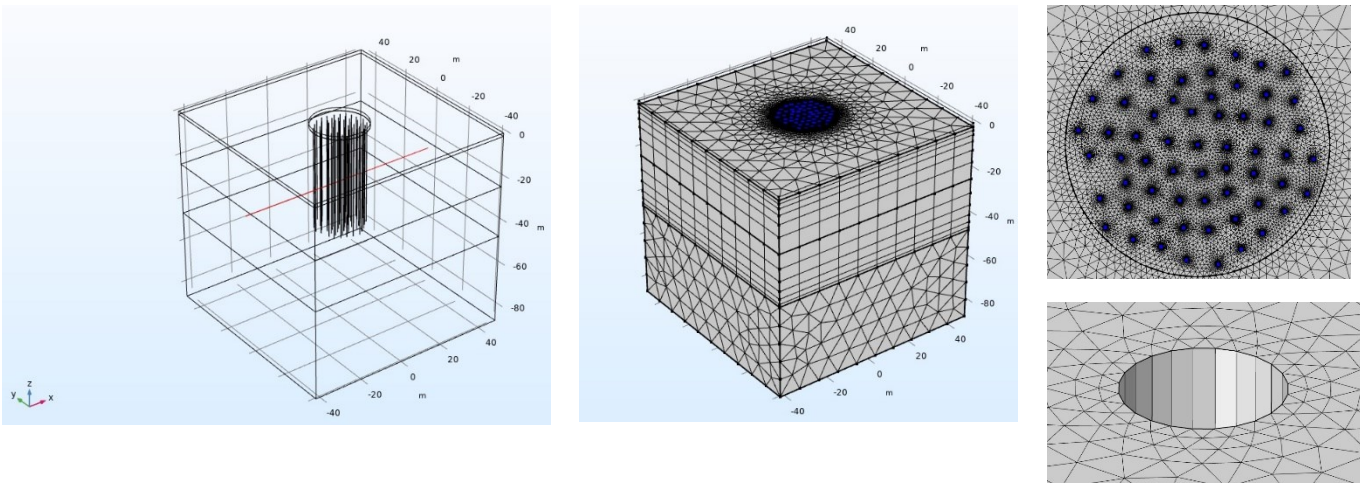

Figure 3: a) 3D-model geometry and cross-section line (red) in the x-direction. Temperature profiles on cross-section line are presented in results paragraph. b) Meshed model geometry and c) BHE locations in horizontal surface and zoomed mesh of the single hollow BHE.

2.5 Governing heat equations

Heat transfer in the ground and in the BHEs is modelled using finite element method. Heat transfer is assumed to be purely conductive without groundwater flow in the subsurface surrounding BHEs. Heat exchange between ground and the BHEs is coupled together using four partial differential equations: one for descending and ascending flows, one for grouting material (groundwater) and one for soil surrounding the BHEs. Heat equations concerning the fluid flow can be written as one dimensional line elements presented by Al-Khoury et al. (2010) and Diersch et al. (2011). This approach however requires that the borehole interior is also meshed. We wrote heat equations (eq. 1-3) as linearly discretized boundary elements in the borehole wall without the need for BHE interior meshing. Used approach was validated against thermal response test interpretations and analytical infinite line source solution.

Heat equations (1) and (2) are used for fluid flows inside collector pipes. Fluid temperatures T_d (downflow) and T_u (upflow) are connected to the grouting material with the heat transfer coefficient b_{fg} ($Wm^{-2}K^{-1}$). Heat exchanger fluid has density ρ_f (kgm^{-3}), specific heat capacity c_f ($Jkg^{-1}K^{-1}$) and thermal conductivity k_f ($Wm^{-1}K^{-1}$). Equation 3 describes heat transfer in the groundwater filled space (temperature T_g) and heat transfer in the subsurface (temperature T_s) is modelled using conductive heat equation (eq. 4). Advection terms (average velocity u) are included only in differential equations concerning fluid flow (equations 1-2) inside pipes as follows,

$$\rho_f C_f \frac{\partial T_d}{\partial t} \mathrm{d}V_p - k_f \nabla^2 T_d \mathrm{d}V_p - \rho_f C_f u \frac{\partial T_d}{\partial z} \mathrm{d}V_p = b_{fg}\left(T_g - T_d\right)\mathrm{d}S_p, \quad (1)$$

where subscript d denotes descending shank and p refers to pipe. Since coupling between groundwater inside the borehole is done using heat transfer coefficient on the collector outer surface then $dV_p = \pi r_i^2 dz$ and $dS_p = 2\pi r_o dz$, where dz is infinitesimal height parameter and r_i (m) and r_o (m) are pipe inner and outer radius, respectively. For ascending flow, the heat equation is:

$$\rho_f C_f \frac{\partial T_u}{\partial t} \mathrm{d}V_p - k_f \nabla^2 T_u \mathrm{d}V_p + \rho_f C_f u \frac{\partial T_u}{\partial z} \mathrm{d}V_p = b_{fg}\left(T_g - T_u\right)\mathrm{d}S_p \quad (2)$$

Heat transfer in groundwater filled space is modelled as a pure conductive heat equation where ρ_g, c_g and k_g are density (kgm^{-3}), specific heat capacity ($Jkg^{-1}K^{-1}$) and thermal conductivity of grout ($Wm^{-1}K^{-1}$), respectively. Coupling with ascending and descending flows is done as follows:

$$\rho_g C_g \frac{\partial T_g}{\partial t} \mathrm{d}V_g - k_g \nabla^2 T_g \mathrm{d}V_g = b_{fg}\left(T_d - T_g\right)\mathrm{d}S_p + b_{fg}\left(T_u - T_g\right)\mathrm{d}S_p + b_{gs}\left(T_s - T_g\right)\mathrm{d}S_g \quad (3)$$

where $\mathrm{d}S_g = 2\pi r_b dz$ with r_b being the borehole radius. Conductive heat transfer equation for subsurface temperature T_s with thermal conductivity k_s is:

$$\rho_s C_s \frac{\partial T_s}{\partial t} + \nabla \cdot (-k_s \nabla T_s) = b_{gs}\left(T_g - T_s\right) \quad (4)$$

where ρ_s is density and c_s is specific heat capacity of subsurface ($Jkg^{-1}K^{-1}$). Heat transfer coefficients b_{fg} (fluid to grout) ($Wm^{-2}K^{-1}$) and b_{gs} (grout to soil) ($Wm^{-2}K^{-1}$) are calculated analytically exploiting thermal resistance equations. Heat transfer coefficient between working fluid and collector outer surface is:

$$b_{fg} = \frac{1}{R_{fg} 2\pi r_o} \quad (5)$$

and coefficient between grout and subsurface is:

$$b_{gs} = \frac{1}{R_{grout} 2\pi r_b} \quad (6)$$

where, R_{grout} is thermal resistance of grout (mKW^{-1}). Thermal resistance of water inside BHEs was calculated as a difference between local borehole thermal resistance and coupled resistance of pipe and working fluid. Local borehole thermal resistance R_b (mKW^{-1}) for both charging and discharging periods was calculated using Multipole –method with first order expression (Javed et al., 2017).

$$R_b = \frac{1}{4\pi k_g}\left[\beta + \ln\left(\frac{\theta_2}{2\theta_1(1-\theta_1^4)^\sigma}\right) - \left(\frac{\theta_3^2\left(1-\frac{4\sigma\theta_1^4}{1-\theta_1^4}\right)^2}{\frac{1+\beta}{1-\beta}+\theta_3^2\left(1+\frac{16\sigma\theta_1^4}{(1-\theta_1^4)^2}\right)}\right)\right] \quad (7)$$

where k_g is the grout (water inside BHE provides the thermal contact between collector and BHE wall) thermal conductivity ($Wm^{-1}K^{-1}$) and

$$\beta = 2\pi k_g R_{fp}, \quad \theta_1 = \frac{s}{2r_b}, \quad \theta_2 = \frac{r_b}{r_o}, \quad \theta_3 = \frac{1}{2\theta_1\theta_2}, \quad \sigma = \frac{k_g - k_s}{k_g + k_s} \quad (8)$$

Shank spacing s (m) represents the distance between middle points of collector shanks. Thermal resistance R_{fp} (mKW^{-1}) is the combination of convective resistance inside pipes and resistance of pipe material.

2.6 Model parameters, initial values and power calculations

Heat transfer by natural convection inside the BHE was considered by increasing the water thermal conductivity to the value of 1.6 $Wm^{-1}K^{-1}$ which is almost three times higher than that of stagnant water. Local borehole thermal resistance calculated using Multipole -method is then approximately 0.08 which represents also the average value of resistance determined from the thermal response tests. The subsurface thermal conductivity was 2.47 $Wm^{-1}K^{-1}$, density 2750 kgm^{-3} and specific heat capacity 945.5 $Jkg^{-1}K^{-1}$. The thermal conductivity value used for 0.1 m Styrofoam layer was 0.05 $Wm^{-1}K^{-1}$, density 40 kgm^{-3} and specific heat capacity 1450 $Jkg^{-1}K^{-1}$. Parameters used for overburden above boreholes were 1.4 $Wm^{-1}K^{-1}$, 2750 kgm^{-3} and 945.5 $Jkg^{-1}K^{-1}$ respectively.

The heat flux boundary condition 40 mW/m^2 was applied to the bottom boundary of the model. Ground surface temperature was fixed to a value of $5.7 + 6.0\sin\left((2\pi/1[a])t\right)$ [°C], with 6.0 °C being the temperature amplitude between yearly average ground surface temperature. No-flux boundary condition was set on the far-field vertical boundaries.

The total flow rate in simulations during charging period was 102.6 dm^3min^{-1} and during discharging period 84.0 dm^3min^{-1}. The total flow rate is divided into each BHE ring in this BTES system. The flow rate per borehole in a certain ring is therefore obtained by dividing the total flow rate with number of BHEs. The flow rate in each of the BHEs in the first ring (8 boreholes) is for example 12.8 dm^3/min during charging period. The charging period power received by each ring, Q_{inj} (W) is calculated as a temperature difference:

$$Q_{inj} = c\rho\dot{V}(T_{in} - T_{out\_j}) \quad (9)$$

where T_{out_j} is the average water outlet temperature either from j=1st, 2nd, 3rd or 4th ring (Fig. 2), T_{in} is 70 °C and $\dot{V}$ is the fluid volumetric flow (m^3).

The extracted heat rate during discharging period, Q_{ext} (W), is calculated:

$$Q_{ext} = c\rho\dot{V}(T_{out\_j} - T_{in}) \quad (10)$$

where T_{in} is 20 °C.

The BTES heat injection rate originates from the compressor waste heat production and the solar panels. Assumption of the duration of continuous heat charging phase was 150 days (24/7) with inlet temperature of 70 °C (inlet to 8 middle BHEs) and heat extraction phase 120 days (24/7) with inlet temperature of 20 °C (inlet to 23 BHES in 4th ring). Simulations were performed for ten charging and discharging periods. The extraction efficiency increases every year because of elevated BTES temperature. The storage efficiency is a relation between extracted and injected energy $\eta = E_{out}/E_{in}$, where E_{out} is extracted and E_{in} injected energy (Schulte, 2016).

2.7 DTS and TERMO sensors field measurements

The optical fiber was connected to the Oryx Sensornet DTS-device (Distributed Temperature Sensing). The cable is BRUsens temperature 85 °C which contains four graded index multimode fibers 50/125 µm inside stainless steel loose tube. Measuring principle of the DTS is based on the Raman scattering effect and temperatures are calculated using a ratio between anti-Stokes and Stokes intensities. Temperatures were determined in one-meter interval from the whole length of the fiber. DTS-temperature profiles were measured in February and in June 2019.

TERMO temperature sensors were installed into 26 boreholes. The number of TERMO cables is eight in the first ring and second, third and fourth ring contains six cables each (Fig. 2). Each cable includes temperature sensors between five-meter intervals and hence there are nine sensors in each borehole. The sensors measure the groundwater temperature continuously inside the boreholes. The first temperature sensor is near the lower surface of the insulation layer.

3. RESULTS

3.1 Initial temperature measurement and Thermal response test

Temperature gradient of the subsurface could not be determined from the measured temperature profiles because of the shallow boreholes (Fig. 4). The temperature profile of the bedrock is rather stable to the depth of 60 m. Thus, the average initial temperature of 5.7 °C was used in the numerical BTES simulations.

The thermal conductivity value obtained from the first TRT-measurement was 2.5 W/(mK). The average effective thermal conductivity of the subsurface from two thermal response tests was 2.47 W/(mK). The effective thermal resistance values interpreted from the TRTs were 0.076 m•K/W (PEH pipe, thickness of the pipe wall 2.3 mm) and 0.086 mK/W (PE-RT, polyethylene of raised thermal resistance with thickened wall (3.7 mm). In the numerical BTES simulations the thermal resistance of the boreholes was however calculated analytically using Multipole-method.

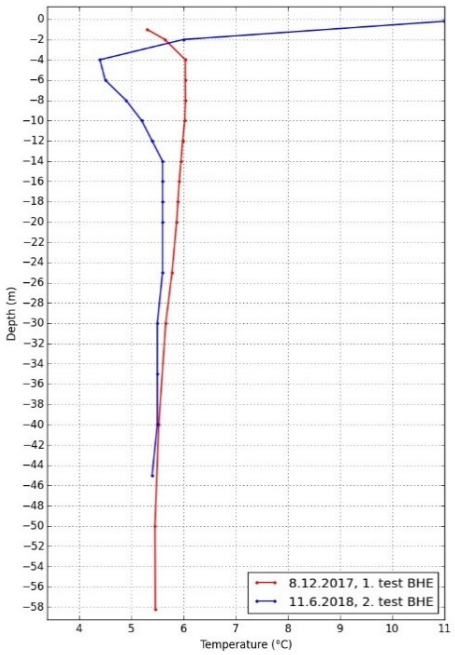

Figure 4: Measured initial temperature profile of the subsurface before TRT measurements.

3.2 Simulation results

The BTES simulations showed that the maximum instantaneous power requirement of 150 kW could be managed with 61 BHEs (depth 45 m) in hexagonal pattern. However, the drilled BTES is not exactly hexagonal as was shown in the Fig. 2 and 3c.

Subsurface temperature will evolve rapidly after charging is started and a maximum temperature close to 67 °C is reached after 150 days at the core of the storage (Fig 5). During the charging period a maximum power is reached if the water outage is from the 4th ring. After 150 days of charging the maximum heat rate is approx. 130 kW. In discharge phase the flow direction is from the 4th ring towards the center of the storage. A maximum power outage is reached if the water outlet is from the 1st ring. After 120 days of discharging the heat rate is approximately 30 kW (Fig 6).

The BTES efficiency is increased after each charging/discharging cycle. The theoretical maximum efficiency after the first cycle assuming no convective heat losses and groundwater flow in the subsurface is (229.9 MWh/763.2 MWh) • 100 % = 30.1 %, where

integrated cumulative energies for each phase are as shown in the Fig. 5. The theoretical BTES efficiencies in the following cycles are 47.2, 52.3, 54.8, 56.4, 57.5, 58.3, 59.0, 59.5 and 59.9 %, respectively.

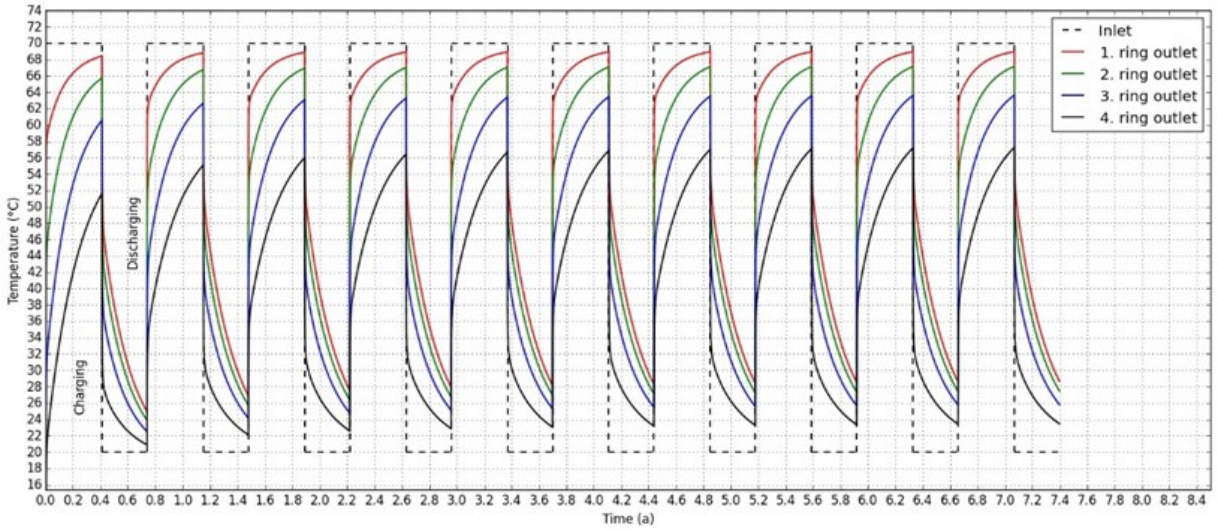

Figure 5. The heat carrier fluid temperature in the outlet from each BHE ring during charging (inlet temperature 70 °C to the eight middle BHEs) and discharging (inlet temperature 20 °C to the 23 BHEs in the 4th ring).

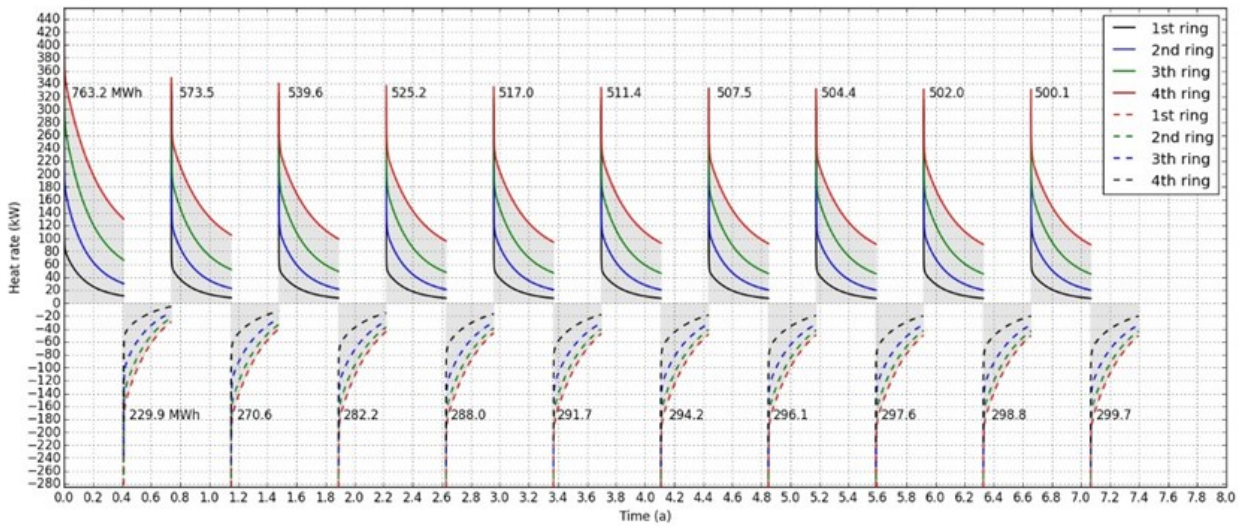

Figure 6. Heat rates (kW) charged to and discharged from the BTES according to the COMSOL simulations.

Figure 7 shows how the subsurface temperature will evolve between the 1st, 5th and 10th charging and discharging cycles in the depth of 25 m in a horizontal cross-section line as shown in the Fig. 3. The last temperature profile after each discharging phase is the same as the initial temperature of the following charging phase. The temperatures are presented for each phase in one-month intervals. One 150-day charging period is enough to rise the storage temperature to the maximum temperature of 67 °C in the center of the storage. During the discharging period the subsurface temperature near the storage center drops to near 30 °C. Figure 8 shows how the temperature front proceeds in the ground as a function of depth between the first, fifth and last simulated charging/discharging cycle. The bedrock temperature beneath the boreholes rises quite significantly during the operating years. The temperature plume does not seem to penetrate deeper than approximately 80 m below the ground surface level (Fig. 8).

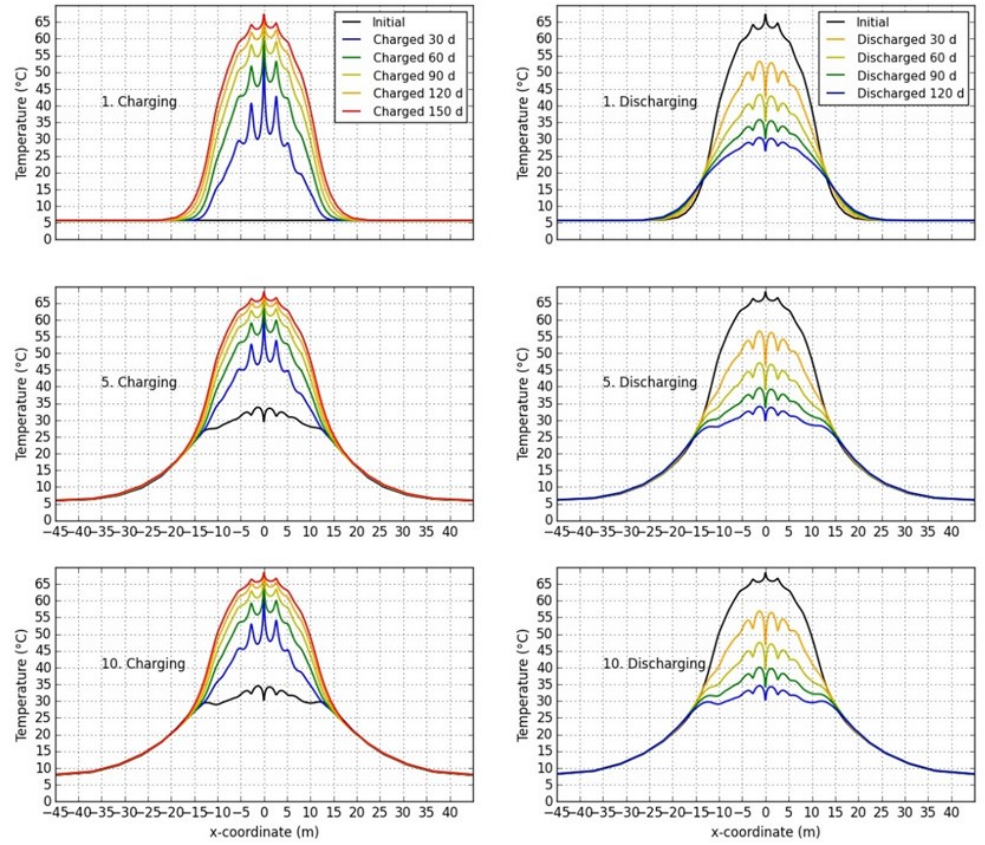

Figure 7. Subsurface temperatures from the depth of 25 m in x-direction for the 1st, 5th and 10th charging/discharging cycles.

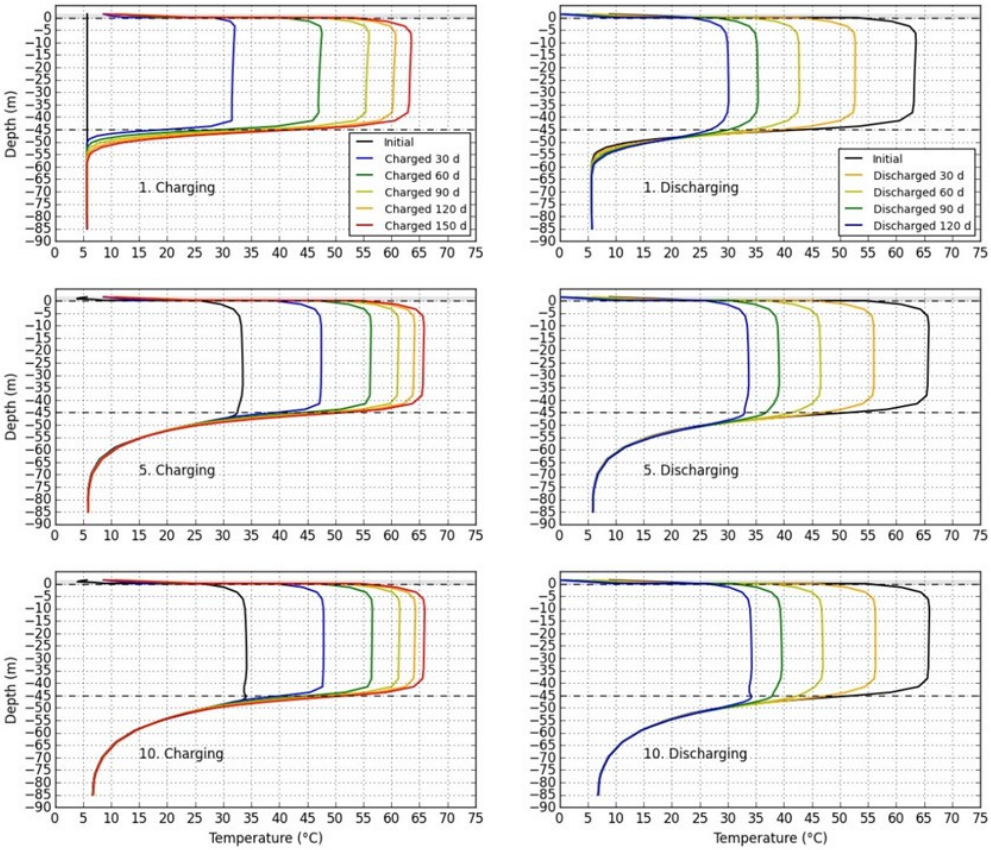

Figure 8. Subsurface temperatures as a function of depth (3D cut line (1.5, 0, 1.5), (1.5, 0, -85.0)) during the 1st, 5th and 10th charging/discharging phases.

3.3 Measured temperatures

A DTS-profile measured in February 2019 shows the initial ground temperature before the heat injection was started. Heat was injected to the first BHE ring only between May-June 2019 and the maximum temperature beneath the insulation near the first ring increased on the level of 27.7 °C. The results from the DTS measurement indicate that the temperature beneath the Styrofoam insulation was higher than on the surface above for both measurements (Fig. 8). The temperature disturbances beneath the insulation show that temperature is higher near the storage center than near the edges of the insulation.

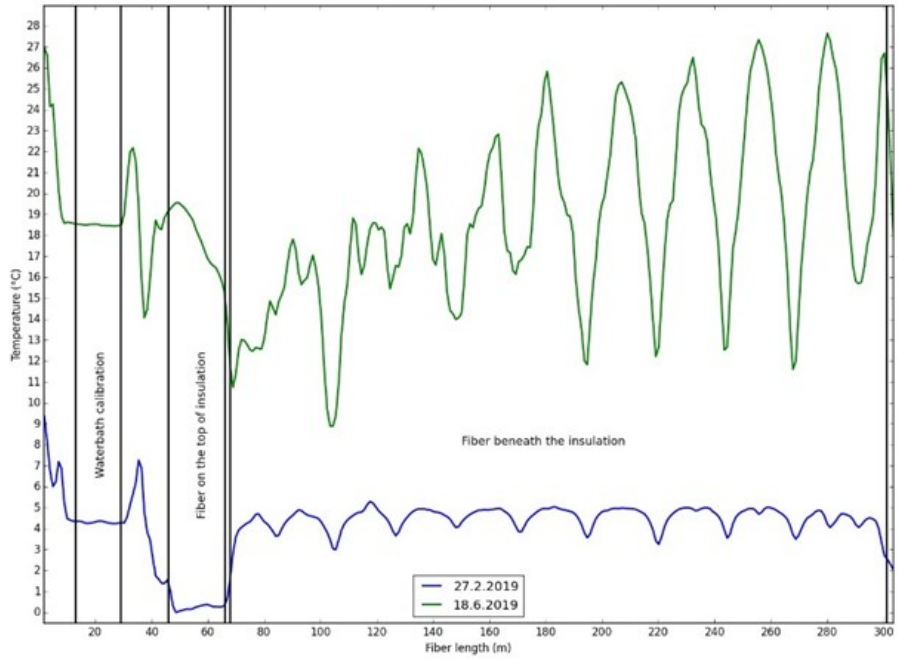

Figure 9. The temperature profiles on the upper and bottom surfaces of the Styrofoam insulation layer.

TERMO sensors indicate that after one month charging period the subsurface temperature is close to 30 °C near the middle BHEs (Fig 10). The subsurface temperature in the 4th ring in the depth of 25 m after one month charging period is close to 11 °C which is little less than simulated value 14 °C. During the spring 2019 it was also noted that not all planned temperature values could be read from TERMO cables. It seems that several sensors may be broken.

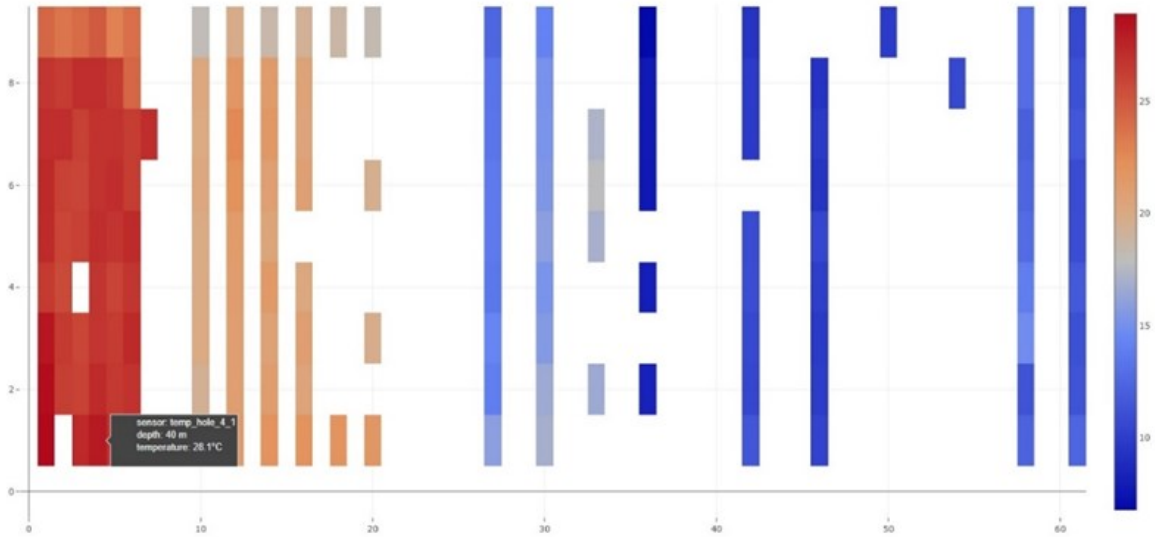

Figure 10. The temperature of the groundwater inside BHEs on 3th June 2019. X-axis denotes the label of the borehole equipped with TERMO cable.

4. DISCUSSION AND CONCLUSION

The results indicate that it is possible to establish a medium or high temperature BTES on harsh climatic conditions like in Central Finland. Storing waste heat to the ground for further utilization reduces greenhouse gas emissions especially if the waste heat utilization replaces the use of fossil fuel. This is the case in the study area. Special attention has to be paid for topsoil insulation, careful system planning, modelling and intelligence operating based on on-line temperature measurements of the BTES. Knowledge of local geological factors is essential for further investigation.

In this project, the optimum BTES construction was to drill 61 boreholes with diameter of 115 mm to the depth of 45 m and with a hexagonal shape. The distance between boreholes is approximately 2.5 m. Furthermore, the BTES is divided into four rings of boreholes which are connected in series. This configuration provides that the temperature may rise approximately to 67 ° in the middle of BTES and it is possible to utilize instantaneous power of 150 kW. Numerical BTES simulations were conducted in total for twenty periods, ten charging phase and ten extraction phases. During step change between charging and discharging flow direction was changed either from the center to the outer boundaries or vice versa. There was no idle period between phases. The simulations showed how the temperature in the subsurface surrounding the BTES should evolve theoretically if the flow rates and the inlet temperatures are set as mentioned.

Optimal spacing between boreholes is critical due to thermal losses. The depth to diameter ratio of this BTES is approximately 1.9. This is in accordance with literature as Ritola (1988) stated that optimal depth to diameter ratio for BTES systems is 1-2 being the highest for small storages. Sibbit and McClenahan (2015) showed that BTES extraction efficiency decreases for storages with high depth to diameter ratio. For low subsurface thermal conductivities borehole spacing could be lower than with high conductivities. This was studied here using COMSOL model with three adjacent boreholes. The temperature between boreholes and near the borehole wall is higher with low thermal conductivity. Also because of high soil specific heat capacity the thermal diffusivity is low. Therefore, the volume of temperature plume is small in soil. In this BTES the subsurface heat capacity is high due to thick soil layer.

Each BHE is filled with groundwater and hence the temperature inside the BHE defines the amount of heat transfer occurring by natural convection. The higher is the water temperature, the smaller is the effective thermal resistance because of enhanced heat transfer inside the BHE. The outlet temperature from the BTES during discharging phase is higher in low flow rate conditions than in high flow rate conditions.

The BTES simulated efficiency arises approximately to 60% after ten years of operation. In the first year, the efficiency is 30.1 % which increases to 56.4 % after the fifth operating year. After fifth year the efficiency increases approximately 1 percent during the next 3 years, being approximately 59% after 8th operating year. Hence, the efficiency will increase during operating years but increasing rate will level during time. In comparison to the other experiments, simulated 60 % efficiency is at the upper limit. Only the pilot high-temperature BTES in Brædstrup, Denmark, has already reached over 60 % efficiency (Schmidt and Sørensen, 2018). Typically, high-temperature BTES systems have reached efficiency of 40-50 % (Sibbitt et al., 2012, Bauer et al., 2016, Nussbicker et al., 2007, Nordell, 1994).

The system building schedule has protracted and hence heat injection to the BTES started from May 2019. The injection rate has not been constant. The field measurements indicate that after one month charging period the subsurface temperature is close to the values predicted by the simulations. The measured temperature values on the peripheral of the BTES are lower than simulated. The measured DTS-profile beneath the insulation is in good accordance with values measured using TERMO cables in June 2019. However, field measurements are only indicative due to short heating period. Short, irregular heating may be the reason for the noticed temperature differences on border of the BTES. It also seems that the TERMO sensors are not working as planned. Hence, there is a need for further field measurements to compare the simulation and the recorded temperature evolution. There is also a need to develop temperature sensors that can tolerate harsh conditions.

It is vital to provide experiences from various underground energy storage projects to increase the use of geothermal energy. Hence, more “lessons learned” reports from different countries are needed in the future.

AKNOWLEDGEMENTS

This project is funded partly by the European Regional Development Fund project EVAKOT (Energian varastoinnin ja käytön optimoinnin työkalut). Project is also included to the European Commission H2020 project ENeRAG (Excellency Network Building for Comprehensive Research and Assessment of Geofluids) program. We thank our supporters. We also want to thank our colleagues form GTK Geoenergy group for the support and help.

REFERENCES

Al-Khoury, R., Kolbel, T. and Schramedei, R.: Efficient numerical modeling of borehole heat exchangers. *Computers & Geosciences*, **36**, (2010). 1301–1315.

Bauer, D., Drück, H., Lang, S., Marx, R., and Plaz, T.: Weiterentwicklung innovativer Technologien zur solaren Nahwärme und saisonale Wärmespeicherung Akronym, Wintersun. Stuttgart, Germany. (2016).

Catolico, N., Ge, S., and McCartney, J.S.: Numerical modelling of a Soil-Borehole Thermal Energy Storage System. *Soil science society of America*, (2015) pp.1-17.

Diersch, H.-J.G., Bauer, D., Heidemann, W., Ruhaak, W. and Schatzl, P.: Finite element modeling of borehole heat exchanger systems. Part 1. Fundamentals. *Computers & Geosciences*, **37**, (2011). 1122–1135.

Dumas, P., Garabetian, T., Serrano, C., and Pinzuti, V.: 2018 EGEC geothermal market report. European geothermal energy council. Brussels. (2019).

ECF. Net zero by 2050: From Whether to how. Zero emissions pathways to the Europe we want. European Climate Foundation. (2018) Accessed 25 June 2019 https://europeanclimate.org/wp-content/uploads/2018/09/NZ2050-full-report-print-version.pdf.

ECF. Towards fossil-free energy in 2050. European Climate Foundation. (2019) Accessed 25 June 2019 https://europeanclimate.org/wp-content/uploads/2019/03/Towards-Fossil-Free-Energy-in-2050.pdf.

ECF. Road Map 2050. A Practical guide to a prosperous low-carbon Europe. Hague, (2010).

Ge, M., Lebling, K., Levin, K., and Friedrich, J.: Tracking progress of the 2020 climate turning point. Working paper. World Resources Institute. Washington DC. (2019). Accessed 25 June 2019 https://wriorg.s3.amazonaws.com/s3fs-public/2020-turning-point-progress_2.pdf.

Hietula, S.: Temperature of shallow groundwater in Finland – the utility of national mapping to estimate geoenergy potential. *Pro Gradu thesis.* University of Helsinki, Department of Geosciences and Geography. (2018) [in Finnish, abstract in English].

Javed, S. and Spitler, J.: Accuracy of borehole thermal resistance calculation methods for grouted single U-tube ground heat exchangers. *Applied Energy*, **187**, (2017). 790-806.

Korhonen, K., Leppäharju, N., Hakala, P. and Arola, T.: Simulated temperature evolution of large BTES – case study from Finland. *Proceedings* of the IGSHPA Research Track, Stockholm September 18-20. (2018). DOI: 10.22488/okstate.18.000033

Lanahan, M., Tabares-Velasco, P.C.: Seasonal thermal-energy storage: A critical review on BTES systems, modeling, and system design for higher system efficiency. *Energies* **10**, (2017), 743–767. https://doi.org/10.3390/en10060743

Nordell, B.: Large-scale thermal energy storage, in: *Proceedings* of Winter Cities, Energy and Environment. Luleå, Sweden. https://doi.org/10.1088/2040-8978/13/5/055203. (2000).

Nordell, B.: Borehole heat store design optimization. *Doctoral thesis*. Luleå University of Technology. https://doi.org/ISSN: 0348-8373. (1994)

Nussbicker, J., Heidemann, W., and Mueller-Steinhagen, H.: Monitoring results and operational experiences for a central solar district heating system with Borehole Thermal Energy Store in Neckarsulm (Germany), in: *EcoStock*: Tenth International Conference on Thermal Energy Storage. Richard Stockton College of New Jersey, Pomona, NJ. (2006).

Ritola, J.: Lämmön varastointi kallioperään. VTT, (1998). Helsinki. ISBN-13: 9789513830960. [in Finnish].

Schmidt, T., Sørensen, P.A.: Monitoring results from large scale heat storages for District Heating in Denmark. *Proceedings* of 14th International Conference on Energy Storage 25-28 April 2018. EnerSTOCK2018. Adana, Turkey. (2018).

Schulte, D.: Simulation and Optimization of Medium Deep Borehole Thermal Energy Storage Systems. *PhD thesis*. TU Darmstadt. (2016).

Shah, S.K., Aye, L., and Rismanchi, B.: Seasonal thermal energy storage system for cold climate zones: A review of recent developments. *Renew. Sustain. Energy Rev*. (2018). https://doi.org/10.1016/j.rser.2018.08.025.

Sibbit, B., and McClenahan, D.: 2015, Seasonal Borehole Thermal Energy Storage – Guidelines for design & construction. *IEA-SCH Tech Sheet* **45.B.3.1**, (2014), 1-15.

Sibbitt, B., McClenahan, D., Djebbar, R., Thornton, J., Wong, B., Carriere, J., and Kokko, J.: 2012. The performance of a high solar fraction seasonal storage district heating system - Five years of operation, in: *Energy Procedia*, **30**, (2012) 856–865. https://doi.org/10.1016/j.egypro.2012.11.097

Valkila, N., and Saari, A.: Urgent need for new approach to energy policy: the case of Finland. *Renewable & Sustainable Energy Reviews*, **14** (2010), 2068–76.

Welsch, B., Ruhaak, W., Schulte, D. O., Bär, K., and Sass, I.: Characteristics of medium deep borehole thermal energy storage, *International journal of Energy Research*, **40**, (2016), 1855-1868.